

3D Radiation Imaging Using Mobile Robot Equipped with Radiation Detector

Doyeon Kim, Hanwool Woo, Yonghoon Ji, Yusuke Tamura, Atsushi Yamashita, and Hajime Asama

Abstract—This paper presents a novel scheme for the three-dimensional (3D) reconstruction of radiation source distribution by using multiple viewpoint of detector. Detecting and localizing radiation source are required for nuclear safety, security, and surveillance when considering exposure to radiation. In such cases, 3D reconstructed information would greatly contribute to a better understanding of the spatial relation between radiation sources and a surrounding environment. Considering contamination of radiation for human, we used a mobile robot equipped with a detector because it is suitable to measure a radiation in multiple viewpoint. We assume that trajectory of the mobile robot with the detector (i.e., pose of the detector) is estimated by simultaneous localization and mapping (SLAM) scheme. Therefore, 3D radiation source distribution can be reconstructed by utilizing maximum likelihood expectation maximization (MLEM) method, which performs optimization based on all measured data and estimated detector poses. The result of the simulation experiment demonstrated that the proposed framework can accurately perform 3D reconstruction of radiation image in the indoor environment.

I. INTRODUCTION

Detecting and localizing radiation sources are important abilities for nuclear safety and security. Generally, a radiation detector is employed to comprehend of radiation sources distribution in the field. By measuring radiation emitted from radiation sources, radiation image system, which defines the distribution of radiation source, is applied in those fields of nuclear material and surveillance of nuclear weapon attack. Moreover, radiation image system is required in the decommissioning of Fukushima Daiichi nuclear power plant which had an accident in 2011 for understanding of contaminated area. Understanding of contaminated area is related to decontamination task of the environment that is an urgent task in order to prevent the damage caused by exposure of radiation. Therefore, study of serving the radiation image, which is defined by the distribution of radiation source, is important.

Several studies have been made on generating radiation image using a detector. Generally, combining radiation detector with additional sensors such as optical camera or LRF (laser rangefinder) which is able to measure a surrounding environment, visualization of 2D (two-dimensional) radiation image is available [1,2]. Moreover, it has been reported that 2D radiation image system using a detector mounted on a helicopter was demonstrated in Fukushima area [3]. However, 2D radiation image are limited in comprehend of locational relationship between sources and objects (i.e., the surrounding

environment). Thus, it is very difficult to estimate accurate position of radiation source in case of using such 2D images.

Jiang et al. developed a system using a detector mounted on helicopter with global positioning system (GPS) sensor to collect the data for decontamination of near Fukushima area. The system produces a radiation source distribution map overlay on the satellite image map by integrating measurement data and GPS information. However, generated 2D radiation image is vulnerable to depth information, since the radiation source localization is constraint on the surface of the earth. Little attention has been given to the locational relationship that radiation sources which are located above or below the surface of the earth. Thus, 3D radiation image is the key to solving the estimating locational relationship between sources and objects. Moreover, Ohno et al. have been researched a system for estimating radiation distribution in Fukushima Daiichi nuclear power plant [4]. The system using a radiation detector mounted on a tracked vehicle, which is operated by remote control developed for an investigation of radiation source. This research also showed the 2D result of radiation imaging because, they put the constraint that the radiation source should be located on the surface on the obstacles that can be observed by the sensor which measures the surrounding environment. Thus, remained problem from the radiation imaging system using a tracked vehicle is quite similar to the problem from the above system using helicopter. However, these studies could not generate accurate image where the radiation source in unobservable environment, for example the sources which are located behind the wall.

Very few attempts have been made at 3D radiation image system. In the centimeter scale of small environment, 3D reconstruction is capable with single viewpoint measurement [5]. On the other hand, in case of a large-scale environment, it is not able to reconstruct all the environment with only single viewpoint. In order to produce the 3D radiation image in large

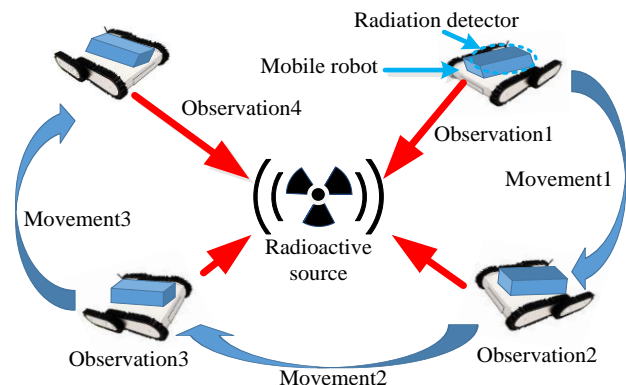


Figure 1. Conceptual image of measuring of radiation source using a detector mounted on a mobile robot.

D. Kim, H. Woo, Y. Ji, Y. Tamura, A. Yamashita, and H. Asama are with the Department of Precision Engineering, School of Engineering, The University of Tokyo, 7-3-1 Hongo, Bunkyo-ku, Tokyo, Japan. {kim, woo, ji, tamura, yamashita, asama}@robot.t.u-tokyo.ac.jp.

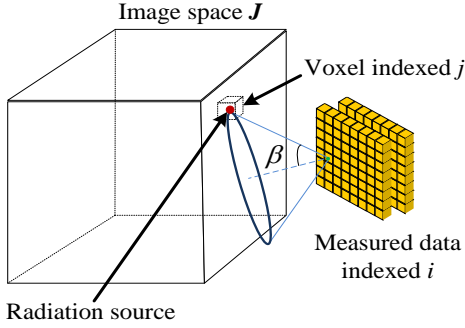


Figure 2. Conceptual image of the 3D reconstruction using measured data which is indexed i in all the measured data D .

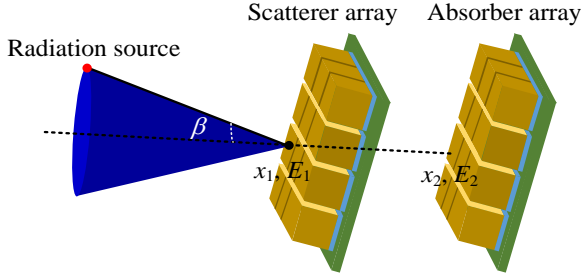


Figure 3. The conceptual image of Compton camera.

environment, it is important to obtain measurement data in multiple viewpoint. R. A. Haefner et al. proposed the 3D gamma-ray imaging system based on SLAM framework using hand-held gamma-ray detector [6]. They demonstrated that 3D source distribution could give spatial information. However, this system requires the near-field observation of source around 1 m away from the detector and the source. Moreover, they used the hand-held detector, which ask a high risk for the observer being contaminated by radioactivity during observation. Therefore, we need to consider the actual applying of system in the contaminated area such as Fukushima Daiichi nuclear power plant.

Our approach is to reconstruct the 3D distribution of the radiation source measured from a detector mounted on a mobile robot in multiple viewpoint in the indoor environment as shown in Fig. 1. First, the mobile robot observes the radiation source at the pose of observation 1. After the first observation is over, it moves to the other pose to measure and stop. The measured data are collected in this way and we assume that the data does not be collected when the mobile robot is moving. In respect to reconstruction process based on the obtained data from the radiation detector, maximum likelihood expectation maximization (MLEM) method, which is widely used in the medical field, is utilized. MLEM can estimate the more accurate position of radiation source in comparison with back-projection which is also the one of general reconstruction method [7,8]. MLEM estimates the position of radiation source by iterative calculation based on the measured data from the detector. In this proposed approach, we assumed that simultaneous localization and mapping (SLAM) scheme [9,10] produces trajectory of mobile robot that equipped with the detector.

The reminder of this paper is organized as follows. Section II briefly introduces the principle of radiation

detection and defines the state variables covered in this study. Section III describes the 3D reconstruction framework which is divided into SLAM and MLEM phases. Section IV discusses the effectiveness of the proposed 3D radiation imaging based on the experimental results. Finally, Section V presents the conclusions.

II. PRINCIPLE OF RADIATION DETECTION

First of all, we will focus our attention on the definition of measured data of the detector. There are many kinds of radiation detector. Generally, the structure of the detector is consist of small detector elements in 2D array as shown in Fig. 2. As the measured data, each elements contains direction information. Because direction information contains a one degree of freedom (DoF) incident angle β of radiation to the detector, it is impossible to estimate accurate direction of radiation source. Thus, a relationship between the measured data set D and the 3D radiation image J which should be produced in this study can be defined as follows:

$$D(i) = T(i; j)J(j) \quad (1)$$

where $D(i)$ denotes all the measured data which contains direction information, the position of detector elements, and the number of measured radiation y_i . Here, i is an index of the detector elements. $J(j)$ is the result of 3D radiation image that contains intensity of radiation source denoted by λ_j . Consequently, after the mobile robot moves around the environment to measure the radiation source, $J(j)$ is calculated using the measured data $D(i)$ and transform matrix $T(i; j) = t_{ij}$ called as system matrix. The system matrix is defined by the geometric structure and physical interaction in the detector. The problem which we have to consider next is finding accurate the system matrix in order to get $J(j)$ by solving the Eq. (1). However, it is impossible to estimate the accurate the system matrix since consideration of noise from detecting and randomness of emission from source are needed.

The detector used for this work is a Compton camera which is known as light-weighted and small radiation detector. In the principle of the Compton camera shown in the Fig. 3, two arrays of detectors which are called scatterer array and absorber array, consist of scintillators. E_1 and E_2 are the energy losses of gamma-ray in two consecutive interaction at the position x_1 on the scatterer array and x_2 on the absorber array. Measurement data of the Compton camera consists with the two interactions x_1 and x_2 and the energy loss E_1 and E_2 of gamma-ray in each array. By calculating those data based on Compton scattering kinematics, the Compton scattering angle which is denoted β in the Fig. 3 is obtained.

III. 3D RECONSTRUCTION

Figure 4 shows overview of the proposed system to obtain 3D radiation image from the reconstruction using the radiation detector mounted on the mobile robot. The process can be divided into two phases: SLAM and MLEM. First, SLAM phase performs to estimate map information and trajectory of the mobile robot based on wheel encoder and range data that measure the surrounding environment; so that each pose of multiple viewpoint can be determined. Next, During MLEM phase, all data list which are composed of detector poses and measurements of the detector 3D radiation imaging are used for optimization to reconstruct in order to obtain 3D radiation

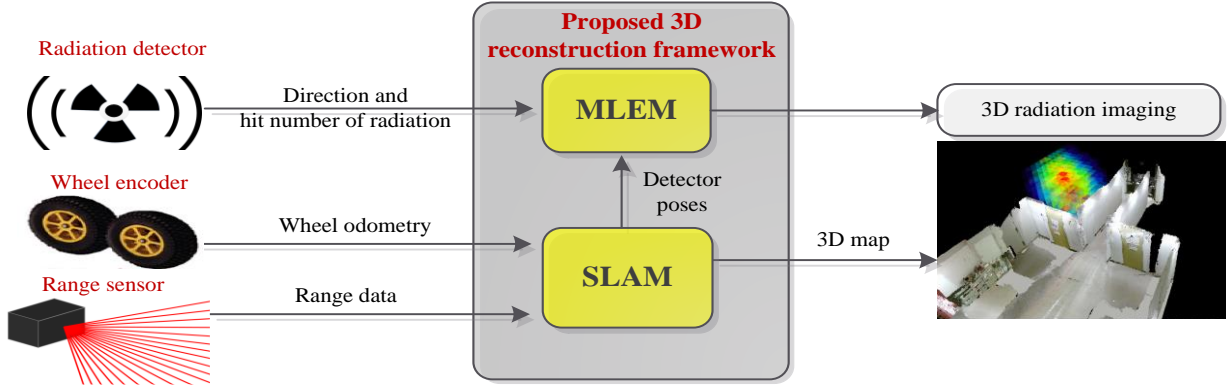


Figure 4. Overview of proposed 3D radiation imaging system using a mobile robot equipped a radiation detector.

image. The details of each phase are described in next subsections.

A. Estimation of Detector poses by SLAM

Before reconstructing the 3D radiation image, each pose of the detector should be estimated in advance given that the number of incident radiation is decided by the geometrical relationship between the source and the detector. In this study, we use a detector mounted on a moving mobile robot to measure radiation in multiple viewpoint; thus, the appropriate pose estimation scheme for the mobile robot should be applied. Furthermore, in order to clearly grasp the positional relationship between the surrounding environment and the 3D radiation distribution, 3D environment model (i.e., map information) also should be built.

Generally, these two problem, localization and mapping, cannot be solved independently. In this respect, we assume that SLAM scheme to estimate the pose of the mobile robot and the surrounding map information at the same time is utilized. Hence, the mobile robot pose and 3D map information can be estimated by integrating sensor data such as wheel encoder and LRF.

B. 3D Reconstruction with MLEM method

It was discussed in section II that the definition of measured data from the detector and the question that we have to solve. As described in Section II, The 3D radiation image $\mathbf{J}(j)$ can be solved by calculating Eq. (1) using measured data $\mathbf{D}(i)$ and the system matrix $\mathbf{T}(i;j)$. Basically, however, it is impossible to get the system matrix easily. The reconstructed image aims to be close to the real one. There are two types of reconstruction method. The basic scheme for the reconstruction is back-projection-based method. However, in general, the large part of reconstructed source distribution contains incorrect information in case of applying the back-projection-based method. For the reconstruction of radiation source distribution, MLEM-based optimization method is also can be used. MLEM is an iterative method for maximizing likelihood function which denotes the likeness of source distribution as follow:

$$\mathbf{L}(\mathbf{J}) = \prod_i p(y_i, \mathbf{J}) \quad (2)$$

$$\mathbf{L}(\mathbf{J}) = \prod_i \frac{Y_i^{y_i} e^{-Y_i}}{y_i!} \quad (3)$$

where $p(y_i, \mathbf{J})$ is the probability that $\mathbf{D}(i)$ contains y_i when the image \mathbf{J} is estimated. Here, we can assume that the probability distribution $p(y_i, \mathbf{J})$ follows Poisson distribution as represented in Eq. (3). Y_i denotes mean value, which can be written as follows:

$$Y_i = \sum_j t_{ij} \lambda_j \quad (4)$$

where t_{ij} is the element of the system matrix $\mathbf{T}(i;j)$ and each element denotes the probability to detect data $\mathbf{D}(i)$ when the radiation emitted from the image $\mathbf{J}(j)$. Then, to find the image \mathbf{J} that maximize Eq. (3) is solved by iterative EM algorithm, which has proven by Barret et al. and Parra and Barret [11,12] as follows:

$$\lambda_j^{(l+1)} = \frac{\lambda_j^{(l)}}{\sum_i t_{ij}} \sum_i t_{ij} \left(\frac{y_i}{Y_i^{(l)}} \right) \quad (5)$$

where $l = 1, 2, 3, \dots$ indicates iteration times.

IV. EXPERIMENTS

A. Reconstruction result on difference of distance

This experiment was demonstrated for the imaging system applying MLEM method with the measured data from multiple observation viewpoints. The detector that we used in this experiment was a Compton camera, which has a lightweight and compact size of detector. The measured data consists with combination of incident detector elements and deposited energy, transformed in the incident angle. We used a Compton camera with one hundred of scintillators ($10 \times 10 \times$

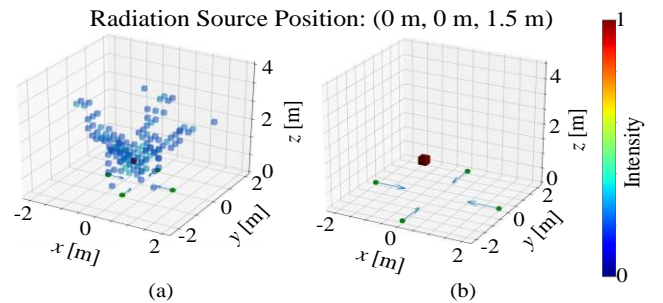


Figure 5. Experimental result of distance 2.5 m: (a) reconstruction result applying simple back projection and (b) reconstruction result applying MLEM of iteration 1.

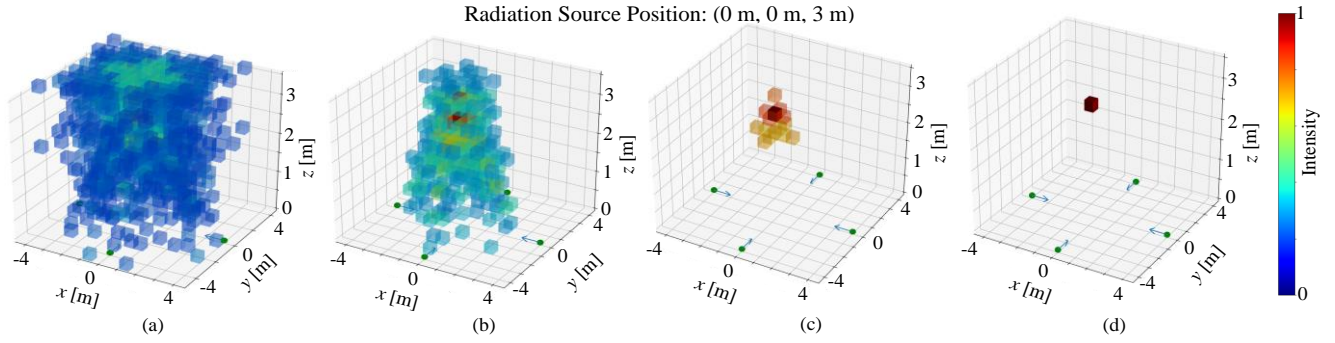


Figure 6. Experimental result of distance 5 m: (a) reconstruction result applying simple back projection, (b) reconstruction result applying MLEM of iteration 1, (c) reconstruction result applying MLEM of iteration 2, and (d) reconstruction result applying MLEM of iteration 3.

10 mm^3) which were coupled to a 10×10 array as the scatterer and absorber. The error events such as back scattering events and multiple scattering which are not proper interaction cases with incident gamma-ray and the Compton camera should be excluded. In our experiment, we knew that the initial gamma-ray energy; thus, it is possible to eliminate effects of those errors mentioned above through the sum of the energy losses in each array.

We conducted two comparative experiments and each measurement data were taken in four places that had same distance between Cs-137 source and the detector. Here, we assumed that each of distances are 2.5 m and 5 m. The measuring Cs-137 using the detector was performed by the Geant4 toolkit [13,14]. Geant4 toolkit is a simulation tool for detailed understanding of particles such as neutron, electron, and ionizing radiation through objects. This toolkit is widely used in nuclear engineering, medical field for inspection using radiation.

The four observation poses of the detector in the distance 2.5 m between the source and the mobile robot were (2 m, 0 m, 0 m, 0 deg, 0 deg, 180 deg), (0 m, 2 m, 0 m, 0 deg, 0 deg, -90 deg), (-2 m, 0 m, 0 m, 0 deg, 0 deg, 0 deg), and (0 m, -2 m, 0 m, 0 deg, 0 deg, 90 deg) which are represented as green dots in the Fig. 5. The orientations of the mobile robot are represented as blue arrows. The radiation source was located at (0 m, 0 m, 1.5 m). The reconstructed result applying back-projection and MLEM with the measured data in case of that the source and the detector are 2.5 m away was represented in Fig. 5. We regularly divided the target space using 0.25 m size voxels. Therefore, the intensity λ_j is estimated based on the center point of each voxel. Here, each value recorded in the voxel were represented by a color distribution. The blue color indicated the lowest value and the red indicated the highest value of the estimated λ_j by reconstruction method. First, Fig. 5 (a) shows the simple back-projection result. In the Fig. 5 (a), the reconstructed intensity values λ_j were distributed near the actual position of radiation source. Next, Fig. 5 (b) shows that the result of reconstruction applying MLEM by the change of iteration from 1. By the iteration of MLEM, the estimated distribution of the radiation source gradually converged to actual position (0 m, 0 m, 1.5 m).

On the other hand, in the case of that the source and the detector are 5 m away, the four poses of the observations for experimental setting were (4 m, 0 m, 0 m, 0 deg, 0 deg, 180

deg), (0 m, 4 m, 0 m, 0 deg, 0 deg, -90 deg), (-4 m, 0 m, 0 m, 0 deg, 0 deg, 0 deg), and (0 m, -4 m, 0 m, 0 deg, 0 deg, 90 deg), which are represented as green dots in the Fig. 6. The orientations of the mobile robot are represented as blue arrows. The orientations of the mobile robot are represented as blue arrows. In this case, the radiation source was located at (0 m, 0 m, 3 m). Figure 6 (a) shows the result of back-projection method. The reconstructed radiation image is scattered in large area and the position of the voxel that has the highest estimated intensity was (0 m, 0 m, 3.5 m). Figs. 6 (b), (c), and (d) shows the MLEM method results. When the iteration time is over 5 times, the radiation image is converged on the single voxel that is located at the actual position of the source (0 m, 0 m, 3 m).

Figure 7 represents the relationship between standard deviation of the estimated distribution which means how much data are scattered and iteration number of the MLEM process. Here, iteration time 0 means reconstructed result by back-projection method. The results clearly show that the reconstructed radiation image is converged to the true position

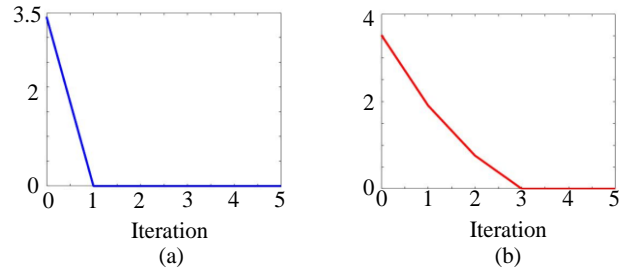


Figure 7. Experimental result of the standard deviation of reconstructed radiation image: (a) the standard deviation graph of distance 2.5 m in the iteration of MLEM and (b) the standard deviation graph of distance 5 m in the iteration of MLEM

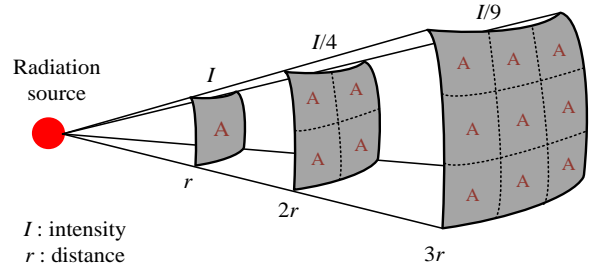


Figure 8. Conceptual image of relationship between detected intensity of radiation and distance.

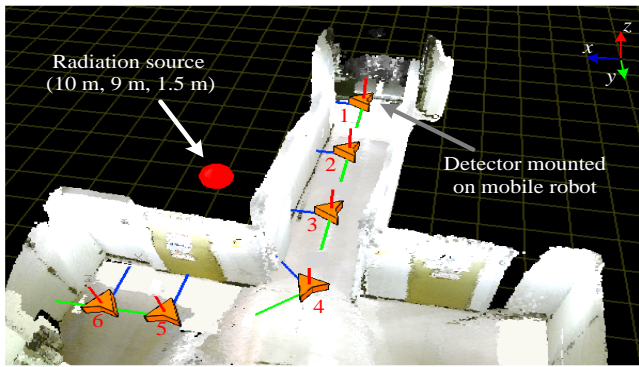


Figure 9. Experimental setting of the radiation source and observation position for detecting radiation source and 3D map of environment.

of radiation source by the increasing of iteration. In addition, comparing with Figs. 7 (a) and (b), the convergence time becomes long if the distance between the source and the detector is far away.

Consequently, when the detector was far from the radiation source, the reconstructed image showed more scattered radiation image and need more iteration time of calculation to be converged on the single voxel. The cause of increase of iteration is due to the decline in the measured number of radiation given that the intensity of radiation becomes weaker as it spreads out from the source as show in Fig. 8. The number of measured radiation is an inverse proportion to the distance from source.

B. Demonstration for the proposed system

The next experiment demonstrated the proposed system assuming the mobile robot equipped the radiation detector. In this experiment, we assumed a Compton camera for a radiation detector and Cs-137 radiation source with the intensity of emission 4000 Bq in the consideration of the measurement time as 5 minutes in each position. Figure 9 shows the experimental environment. Here, the 3D environmental map was generated by the SLAM scheme using the mobile robot equipped with a LRF and encoder in advance. Based on this 3D map information, the radiation which is emitted from the Cs-137 radiation source, was generated by Geant4 toolkit in simulated environment. The true position of radiation source was located in the small room which could not be observed by the LRF, since the door was closed, as shown in Fig. 9. The single grid size is $1\text{ m} \times 1\text{ m}$ in the Fig. 9 and the robot observed the source at six locations near the door, which are presented in the number 1 to 6. Since the radiation source was located behind the door, the true position is presented in the outside of the 3D map. The true orientation

of the detector for each observation are represented by the red, green, and blue color of axes. The blue axis is normal vector of detector face. The poses of the detector as the result of SLAM were set as follows: (8 m, 5 m, 0.5 m, 0 deg, 0 deg, 0 deg), (7.998 m, 6.98 m, 0.499 m, -0.89 deg, -0.15 deg, -1.95 deg), (7.998 m, 8.88 m, 0.499 m, -0.41 deg, -0.25 deg, -44.76 deg), (7.998 m, 10.98 m, 0.499 m, 0.25 deg, 0.53 deg, -90.93 deg), (9.98 m, 10.97 m, 0.49 m, 0.53 deg, 0.28 deg, -90.34 deg), and (10.98 m, 10.97 m, 0.499 m, -0.42 deg, 1.09 deg, -87.85 deg). The true location of the radiation source was set at (10 m, 9 m, 1.5 m). The mobile robot stopped at each observation position while the detector observed the radiation.

In the process of 3D reconstruction using MLEM process, $0.5\text{ m} \times 0.5\text{ m} \times 0.5\text{ m}$ sized voxel were composed of the reconstructed image space. The results of the back-projection and the MLEM process are shown in Fig. 10. Figure 10 (a) is the result applying simple back-projection for the 3D radiation imaging reconstruction. The result shows that the scattered radiation image in the whole environmental area including the corridor and the hall which has no radiation source. Moreover, voxels represented in red color, are estimated in the not only nearest place from the true position of radiation source and but also the other places. Figures 10 (b), (c) and (d) show the reconstructed 3D radiation image by MLEM in the iteration 1, 5, and 10. The results show that the radiation image is converged near the true position of radiation source by the increase of iteration. Especially, Fig. 10 (c) shows that the radiation image is concentrated beyond the wall where almost close to the true position.

Consequently, the result shows that the system is able to generate 3D radiation image, which contains more accurate and intuitive spatial information between radiation source and the surrounding environment compared with the formal research mentioned in the section I. As same as the result from simulation experiment mentioned in subsection VI.A, the image is converged near the radiation source by increasing iteration of MLEM. The position of the voxel that contains highest value of estimated intensity of radiation is (11.5 m, 7 m, 0.5 m) at the result of iteration 10. Compared the true position of the radiation source (10 m, 9 m, 1.5 m), small estimation error occurred. This error is caused by two factors: the uncertainties of detector poses and lack of measured data. First, the detector poses are estimated by SLAM process. In other words, 3D radiation image was reconstructed based on the detector pose with the error. Next, in the light of the results of experiment described in subsection VI.A, the result of the error in the estimation of radiation source is caused by the number of measured data.

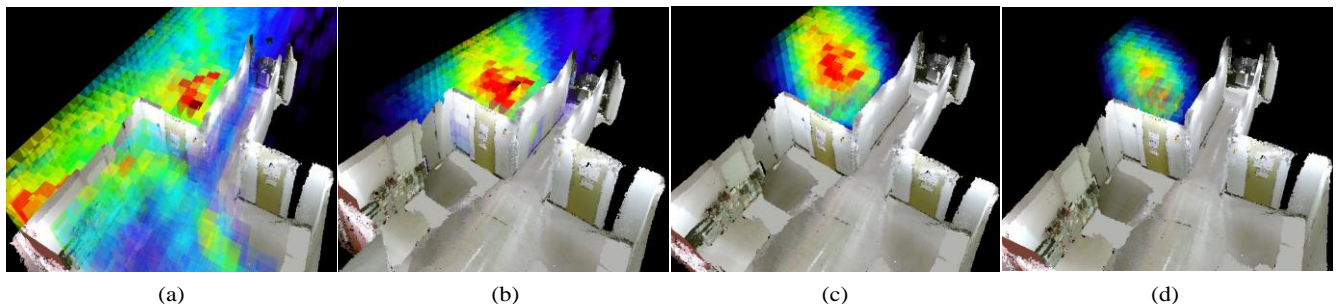


Figure 10. Experimental result: (a) result reconstructed by simple back-projection, (b) result reconstructed by MLEM with the iteration 1, (c) result reconstructed by MLEM with the iteration 5, and (d) result reconstructed by MLEM with the iteration 10.

V. CONCLUSION

In this paper, 3D reconstruction for radiation image using a radiation detector mounted on a mobile robot is proposed. In order to achieve 3D radiation image, SLAM and MLEM method is applied using the measurement data which is obtained at the multiple viewpoint. Thus, the proposed system is able to produce accurate and intuitive information of radiation source position compared with the conventional imaging system.

Two experiments were performed to demonstrate a validity of the proposed system. The first experiment indicates that the accuracy of the reconstruction result is related with the number of measured data since we demonstrated it by changing the distance between the source and the detector. The second experiment showed that our system could estimate the accurate radiation image in the condition of the source being blocked by the obstacle. Thus, our system can produce more accurate and intuitive information of radiation source position compared with the conventional system which reconstructs the radiation image under constraint that the source should be on the surface of obstacles.

ACKNOWLEDGMENT

A part of this study is the result of “HRD for Fukushima Daiichi Decommissioning based on Robotics and Nuclide Analysis” carried out under the Center of World Intelligence Project for Nuclear S&T and Human Resource Development by the Ministry of Education, Culture, Sports, Science and Technology of Japan.

REFERENCES

- [1] C. G. Wahl, W. R. Kate, W. Wang, F. Zhang, J. M. Jaworski, A. King, Y. A. Boucher, and Z. He, “The Polaris-H Imaging Spectrometer,” *Nuclear Instruments and Methods in Physics Research Section A: Accelerators, Spectrometers, Detectors and Associated Equipment*, Vol. 784, pp. 377–381, 2015.
- [2] S. Takeda, A. Harayama, Y. Ichinohe, H. Odaka, S. Watanabe, T. Takahashi, H. Tajima, K. Genba, D. Matsuura, H. Ikebuchi, Y. Kuroda, and T. Tomonaka, “A Portable Si/CdTe Compton Camera and Its Applications to the Visualization of Radioactive Substances,” *Nuclear Instruments and Methods in Physics Research Section A: Accelerators, Spectrometers, Detectors and Associated Equipment*, Vol. 787, pp. 207–211, 2015.
- [3] J. Jiang, K. Shimazoe, Y. Nakamura, H. Takahashi, Y. Shikaze, Y. Nishizawa, M. Yoshida, Y. Sanada, T. Torii, M. Yoshino, S. Ito, T. Endo, K. Tsutsumi, S. Kato, H. Sato, Y. Usuki, S. Kurosawa, K. Kamada, and A. Yoshikawa, “A Prototype of Aerial Radiation Monitoring System Using an Unmanned Helicopter Mounting a GAGG Scintillator Compton Camera,” *Journal of Nuclear Science and Technology*, Vol. 53, No. 7, pp. 1067–1075, 2016.
- [4] K. Ohno, S. Kawatsuma, T. Okada, E. Takeuchi, K. Higashi, and S. Tadokoro, “Robotic Control Vehicle for Measuring Radiation in Fukushima Daiichi Nuclear Power Plant,” *Proceedings of the IEEE International Symposium on Safety, Security, and Rescue Robotics*, pp. 38–43, 2011.
- [5] S. R. Tornga, M. W. R. Sullivan, and J. P. Sullivan, “Three-Dimensional Compton Imaging Using List-mode Maximum Likelihood Expectation Maximization,” *IEEE Transactions on Nuclear Science*, Vol. 56, No. 3, pp. 1372–1376, 2009.
- [6] A. Haefner, R. Barnowski, P. Luke, M. Amman, and K. Vetter, “Handheld Real-time Volumetric 3-D Gamma-ray Imaging,” *Nuclear Instruments and Methods in Physics Research Section A: Accelerators, Spectrometers, Detectors and Associated Equipment*, Vol. 857, pp. 42–49, 2017.
- [7] S. Singh, M. K. Kalra, S. DO, J. B. Thibault, J. B. Pien, H. Connor, and M. A. Blake, “Comparison of Hybrid and Pure Iterative Reconstruction Techniques with Conventional Filtered Back Projection: Does Reduction Potential in The Abdomen,” *Journal of Computer Assisted Tomography*, Vol. 36, No. 3, pp. 347–353, 2012.
- [8] S. J. Wilderman, N. H. Clinthorne, J. A. Fessler, and W. L. Rogers, “List-mode Maximum Likelihood Reconstruction of Compton Scatter Camera Images in Nuclear Medicine,” *Proceedings of the IEEE Nuclear Science Symposium*, pp. 1716–1720, 1998.
- [9] S. Thrun, W. Burgard, and D. Fox, “Probabilistic Robotics,” *MIT Press*, 2005.
- [10] H. Durrant-Whyte and T. Bailey, “Simultaneous Localization and Mapping: Part I,” *IEEE Robotics & Automation Magazine*, Vol. 13, No. 2, pp. 99–110, 2006.
- [11] H. H. Barrett, T. White, and L. C. Parra, “List-mode likelihood,” *Journal of the Optical Society of America A*, Vol. 14, No. 11, pp. 2914–2923, 1997.
- [12] L. Parra and H. H. Barrett, “List-mode Likelihood: EM Algorithm and Image Quality Estimation Demonstrated On 2-D PET,” *IEEE Transactions on Medical Imaging*, Vol. 17, No. 2, pp. 228–235, 1998.
- [13] S. Agostinelli, et al., “GEANT4-A Simulation Toolkit,” *Nuclear Instruments and Methods in Physics Research Section A: Accelerators, Spectrometers, Detectors and Associated Equipment*, Vol. 506, No. 3, pp. 250–303, 2003.
- [14] J. Allison, et al., “Geant4 Developments and Applications,” *IEEE Transactions on Nuclear Science*, Vol. 53, No. 1, pp. 270–278, 2006.